

# Optimal quantum parameter estimation in a pulsed quantum optomechanical system

Qiang Zheng<sup>1, 2</sup>, Yao Yao<sup>1, 3</sup>, and Yong Li<sup>1, 4</sup>

<sup>1</sup> *Quantum Physics and Quantum Information Division,*

*Beijing Computational Science Research Center, Beijing 100084, China*

<sup>2</sup> *School of Mathematics and Computer Science, Guizhou Normal University, Guiyang, 550001, China*

<sup>3</sup> *Microsystems and Terahertz Research Center, China Academy of Engineering Physics, Chengdu Sichuan 610200, China*

<sup>4</sup> *Synergetic Innovation Center of Quantum Information and Quantum Physics, University of Science and Technology of China, Hefei, Anhui 230026, China*

We propose that a pulsed quantum optomechanical system can be applied for the problem of quantum parameter estimation, which targets to yield higher precision of parameter estimation utilizing quantum resource than that using classical methods. Mainly concentrating on the quantum Fisher information with respect to the mechanical frequency, we find that the corresponding precision of parameter estimation on the mechanical frequency can be enhanced by applying applicable optical resonant pulsed driving on the cavity of the optomechanical system. Further investigation shows that the mechanical squeezing resulting from the optical pulsed driving is the quantum resource used in optimal quantum estimation on the frequency.

PACS numbers: 42.50.Wk; 06.20.Dk; 42.50.Pq; 03.65.Yz; 07.10.Cm

## I. INTRODUCTION

Quantum metrology [1] is an active research field in recent years. According to the quantum Cramér-Rao inequality, the quantum Fisher information (QFI) plays a key role in this subject [2–6], which bounds the minimal variance of the unbiased estimator. The QFI gives the quantum limit to the accuracy of the estimated parameter with any positive-operator-valued-measure measurement. One of the central ideas of quantum metrology is to beat the shot-noise limit and approach the Heisenberg limit by virtue of quantum resource, such as quantum entanglement or squeezing. There have been many studies on precision of parameter estimation with sub-shot-noise limit in different physical systems, such as the optical interferometers [7–9], Bose-Einstein condensates [10], atomic interferometers [11], and solid-state systems (e.g., the nitrogen-vacancy centres) [12, 13]. To the best of our knowledge, only a few papers [14–16] have devoted to investigating the quantum metrology in the newly-developed novel quantum optomechanical device.

With the rapid advance of technology, quantum cavity optomechanics [17–19], in which the mechanical resonator is coupled to the optical field by radiation pressure or photothermal force, has excited a burst of interest [20] due to the following two reasons: On one hand, the cavity optomechanical system provides a new platform to investigate the fundamental questions on the quantum behavior of macroscopic system [21] and even the quantum-to-classical transition [22, 23]; On the other hand, it brings a novel quantum device for applications in ultra-high precision measurement [24–28], gravitation-wave detection [29], quantum information processing [30] and quantum illumination [31]. Many interesting researches in cavity optomechanical systems, such as optomechanically induced transparency [32, 33], ground-state cooling of the mechanical resonator [34–38], optomechanical entanglement [39, 40], optimal state estimation [41], have been reported. These studies mainly rely on the enhanced coupling strength between the phonic and photonic fields by strongly pumping the optical cavity with a continuous wave

(CW) laser.

Different from the above case of CW laser driving, the so-called pulsed quantum optomechanics [42], is also realized by driving the optical cavity with (very) short optical pulses. Originally, this strategy has been proposed in the systems of qubits [43], and lately extended to atomic ensembles [44] and levitated microspheres trapped in an optical cavity [45]. Compared with the CW-laser-driving case, the benefit of the pulsed scheme is that it does not need the existence of a stable steady-state for the optomechanical system. The pulsed interaction has also displayed its superiority in preparation and reconstruction of quantum state of the mechanical resonator [46, 47], enhancing the optomechanical entanglement [48, 49] and EPR steering [50], and cooling the mechanical mode [51, 52].

Inspired by the experimental progress in pulsed quantum optomechanical systems [42, 49, 51], it is a natural idea to investigate the high precision of parameter estimation by applying applicable optical pulsed driving on the cavity of the optomechanical system. Here we investigate a special pulsed optomechanical system, where the coupling between the mechanical mode and cavity field is quadratical to the mechanical motion and the cavity field is resonantly driven with external optical pulses. We mainly focus on the QFI with respect to the mechanical frequency, which is equivalent to estimating on the mass of the mechanical resonator and could be used for mass precision detection. With the Cramér-Rao inequality, a larger QFI implies that the mechanical frequency can be estimated with a higher precision. We show that the QFI can be greatly enhanced when the period of the driving pulse matches that of the mechanical motion. We also show that the mechanical squeezing resulting from the resonant driving pulses is the quantum resource strengthening the QFI.

This paper is organized as follows. The pulsed quantum optomechanical model is discussed in Sec. II. We investigate in Sec. III the QFI of the pulsed quantum optomechanical system with respect to the mechanical frequency. Then, we display that the quantum squeezing is the resource used in optimal quantum estimation. Finally, a summary is given in the last

section. The basic properties of the QFI, especially the QFI of a single-mode Gaussian state, are reviewed in Appendix A.

## II. THE PULSED QUANTUM OPTOMECHANICS

Optomechanical systems have been implemented in many physical systems, such as suspended mirrors in the Fabry-Pérot resonators [53], toroidal whispering gallery mode resonators [54], trapped levitating nanoparticles [55], ultra-cold atomic clouds in cavities [56]. Here we focus on a membrane-in-the-middle cavity optomechanical setup [57], which has been used for quantum nondemolition measurement of the phonon number state [58], cooling of mechanical resonator [59] or investigation of Landau-Zener-Stückelberg dynamics [60]. The linear and quadratical optomechanical couplings between the cavity mode and the mechanical resonator can exist in this membrane-in-the-middle optomechanical system. Very recently, the optomechanical quadratical coupling is also achieved in a crystal optomechanical system [61], except for the membrane-in-middle setup.

The membrane-in-the-middle quadratical coupling setup under consideration is shown in Fig. 1 and the corresponding Hamiltonian is expressed as [62]

$$H = \frac{\hbar\omega_m}{2}(\hat{p}^2 + \hat{q}^2) + \hbar\omega_c\hat{a}^\dagger\hat{a} + \hbar g_2\hat{a}^\dagger\hat{a}\hat{q}^2 + i\hbar[E_0(t)e^{-i\omega_d t}\hat{a}^\dagger - h.c.]. \quad (1)$$

Here  $\omega_m$  is the frequency of the mechanical resonator,  $\hat{p}$  and  $\hat{q}$  are the dimensionless momentum and position operators satisfying the relationship  $[\hat{q}, \hat{p}] = i$ ,  $\hat{a}$  is the annihilation operator of the cavity mode with resonance frequency  $\omega_c$  and decay rate  $\kappa$ , and  $g_2$  is the quadratic optomechanical coupling strength. Finally,  $E_0(t) = \sqrt{2P_0(t)\kappa}/(\hbar\omega_c)$  with  $P_0(t)$  the optical input power. We further assume that the cavity is driven resonantly with  $\omega_d = \omega_c$ .

For the mechanical resonator, by linearizing the optomechanical coupling, the corresponding quantum Heisenberg-Langevin equation is obtained as

$$\begin{aligned} \frac{d}{dt}\hat{q} &= \omega_m\hat{p}, \\ \frac{d}{dt}\hat{p} &= -\tilde{\omega}_m(t)\hat{q} - \gamma_m\hat{p} + \xi, \end{aligned} \quad (2)$$

where  $\tilde{\omega}_m(t) = \omega_m + A(t)$  with  $A(t) = 2g_2n_a(t)$  and  $n_a(t) = \langle\hat{a}^\dagger\hat{a}\rangle$ . Here  $\gamma_m$  is the mechanical damping rate, and  $\xi$  denotes for the Brownian noise with null mean and correlation functionsatisfying  $\langle\xi(t)\xi(t')\rangle = 2n_{th}\gamma_m\delta(t-t')$  in the high-temperature limit  $k_B T \gg \hbar\omega_m$ . Here  $k_B$  is the Boltzmann constant,  $T$  is the temperature of the mechanical resonator, and  $n_{th} = [e^{\hbar\omega_m/(k_B T)} - 1]^{-1} \approx k_B T/(\hbar\omega_m)$  is the thermal mean phonon number.

From Eqs. (2), the dynamics of the second order moments of the mechanical system

$$\vec{v}(t) \equiv (\langle\hat{q}^2\rangle, \langle\hat{p}\hat{q} + \hat{q}\hat{p}\rangle/2, \langle\hat{p}^2\rangle)^T \quad (3)$$

can be fully described by the equations

$$\frac{d}{dt}\vec{v}(t) = \mathbf{U}_A\vec{v}(t) + \vec{N} \quad (4)$$

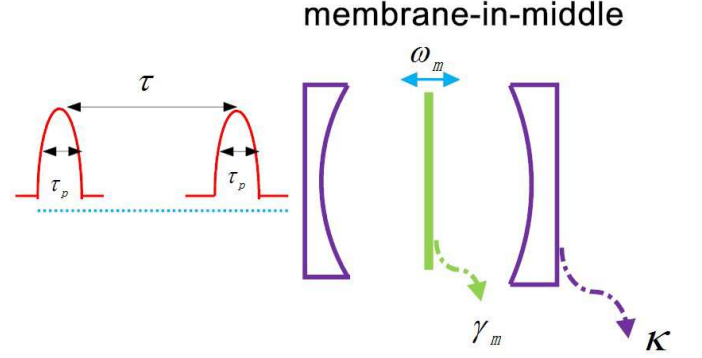


FIG. 1: (Color online) Schematic diagram of the membrane-in-middle cavity optomechanical setup considered in this paper. The coupling between the cavity field (with the decay rate  $\kappa$ ) and the mechanical resonator (with the resonance frequency  $\omega_m$  and the damping rate  $\gamma_m$ ) is quadratical to the mechanical motion, and the driving field is composed by a series of periodic pulses. The duration of one pulse is  $\tau_p$ , and the two consecutive pulses has the time interval  $\tau$ .

for an initial Gaussian state of the mechanical resonator (such as the thermal equilibrium state with mean phonon number  $n_{th}$ ). Here the superscript T represents the transposition. Here

$$\mathbf{U}_A = \begin{pmatrix} 0 & 2\omega_m & 0 \\ -\tilde{\omega}_m & -\gamma_m & \omega_m \\ 0 & -2\tilde{\omega}_m & -2\gamma_m \end{pmatrix}, \quad (5)$$

and  $\vec{N} = (0, 0, (2n_{th} + 1)\gamma_m)^T$ .

The solution of Eq. (4) is formally expressed as

$$\begin{aligned} \vec{v}(t) &= e^{\mathbf{U}_A t}\vec{v}(0) + \int_0^t e^{\mathbf{U}_A(t-t')}\vec{N} dt' \\ &= \mathbf{M}_A(t)\vec{v}(0) + \vec{v}_{\text{inh}}. \end{aligned} \quad (6)$$

Here  $\mathbf{M}_A(t) = e^{\mathbf{U}_A t}$  and  $\vec{v}_{\text{inh}} = \mathbf{U}_A^{-1}[\mathbf{I}_3 - \mathbf{M}_A(t)]\vec{N}$  with  $\mathbf{I}_3$  being  $3 \times 3$  unitary matrix.

Now, we study the case that the driving field is the periodic Gaussian pulses with the duration  $\tau_p$  and period  $\tau$ , i.e.  $P(t) = P_0 \sum_n \exp[-(t - n\tau)^2/\tau_p^2]$ . Here we keep the condition  $1/\tau_p < c/2L$  ( $L$  is the cavity length), which means the optical driving pulses will not excite the near cavity modes except the desired one and thus the cavity field can be always considered as a single mode one. For remaining the quadratic coupling during the pulsed driving, the membrane should be locked at a cavity node. Accordingly the effective frequency of the mechanical resonator is periodically modulated in time via the optical driving pulses. An alternative scheme to achieve periodic modulation of the effective frequency of the mechanical resonator is given in Ref. [63] with a two-tone drive.

Moreover, we assume that the system works in the following parameter regimes: (i)  $1/\tau \ll \kappa$ , (ii)  $1/\tau_p \ll \kappa$ , (iii)  $\tau_p \ll 1/\omega_m$ . The condition (i) implies the cavity is rapidly excited by one pulse and damps to the vacuum state before the next pulse arrives [46]. And the condition (ii) means that the bandwidth of the pulses is much smaller than that of the cavity,

which guarantees the pulse entering into the cavity spectrally. The last condition (iii) makes sure that the free rotation of the mechanical resonator is frozen in the process of the pulse-mirror interaction. In this case, the intracavity photon number can be approximated as a series of Dirac delta functions  $n_a(t) \propto \sum_{n=0} \delta(t - n\tau)$  in the typical evolution time of the mechanical resonator. As a result, the whole dynamics of the optomechanical system is divided into two steps: (1) one kick at time  $t = n\tau$ , which can be described by the unitary operator  $U_K = e^{-i\theta\hat{q}^2}$  with  $\theta = g_2 \int_{\Delta t} n_a(t) dt$  being the kick strength ( $\Delta t$  means the integral time domain and is of the order of the typical time for a Gaussian pulse) and thus corresponds to the linear transformation  $q \rightarrow q$  and  $p \rightarrow p - 2\theta q$ , and (2) the free-evolution lasting time  $\tau$  between two adjacent kicks, whose corresponding evolution is determined by Eq. (2) with  $A(t) = 0$ .

Combined these two evolving processes, the equation of motion in a  $\tau$  circle is given as [46]

$$\vec{v}((n+1)\tau) = \mathbf{M}_0(\tau)\mathbf{K}\vec{v}(n\tau) + \vec{v}_{\text{inh}}(\tau), \quad (7)$$

where  $\mathbf{M}_0(\tau) \equiv \mathbf{M}_{A=0}(t)|_{t=\tau}$ , and

$$\mathbf{K} = \begin{pmatrix} 1 & 0 & 0 \\ -2\theta & 1 & 0 \\ 4\theta^2 & -4\theta & 1 \end{pmatrix} \quad (8)$$

denoting the effect of the kick on the second order moments. That is,  $\mathbf{K}$  is the representation of  $U_K$  based on the second order moments. Making use of Eq. (7), the stroboscopic state of the mechanical resonator at time  $t = n\tau$  is obtained as

$$\begin{aligned} \vec{v}(n\tau) &= (\mathbf{M}_0(\tau)\mathbf{K})^n \vec{v}(0) \\ &+ [\mathbf{I}_3 - (\mathbf{M}_0(\tau)\mathbf{K})^n] (\mathbf{I}_3 - \mathbf{M}_0(\tau)\mathbf{K})^{-1} \vec{v}_{\text{inh}}(\tau). \end{aligned} \quad (9)$$

### III. QFI OF THE PULSED OPTOMECHANICS

After detailed presentation of the pulsed quantum optomechanical model in the previous section, here we move to investigate the quantum parameter estimation via the related QFI in this model. We will also show that the quantum resource used for parameter estimation is the squeezing produced by pulsed driving.

#### A. Primary discussions

The parameter to be estimated in this paper is the frequency  $\omega_m$  of the (harmonic) mechanical resonator. Choosing this parameter is based on the following consideration. With the relation  $\omega_m = \sqrt{k_m/M}$  ( $k_m$  and  $M$  being the spring constant and the mass, respectively), the QFI with respect to  $M$  is proportional to that of with respect to  $\omega_m$ , that is

$$F_M = \mu F_{\omega_m}, \quad (10)$$

where  $\mu = \frac{k_m}{4M^3}$  is the scaling factor. As a result, the estimation on  $M$ , just as done in the mass spectrometer [64], is

equivalent to the estimation on  $\omega_m$ . In principle, the parameter to be estimated in this model can be the ones other than  $\omega_m$  ( $m$ ). Here we just concentrate on the case of  $\omega_m$  via its related QFI  $F \equiv F_{\omega_m}$ .

The numerical values of the parameters used in this paper are based on the state-of-the-art experiments reported in Ref. [65]. We choose the cavity decay as  $\kappa \simeq 10^2$  GHz, and the driving pulses with duration  $\tau_p = 0.1$  ns. We also set the mechanical frequency  $\omega_m = 0.5 \times 10^6$  Hz and the damping rate  $\gamma_m = 10^2$  Hz unless otherwise stated. By carefully choosing the mechanical mass, reflectivity, and initial equilibrium position, the kick strength  $\theta$  is in the range of (0.01, 10) for the typical coupling strength  $g_2$ .

#### B. Numerical results of the QFI

With substituting Eq. (9) into Eq. (A10), the QFI  $F$  can be obtained straightforwardly. Fortunately, the last term in Eq. (A10) vanishes since there is no first-order moment of the mechanical motion. In what follows, we mainly explore  $F$  by numerical simulations as the analytical solution is too cumbersome.

With the extensive numerical simulations, we find that the evolution of  $F$  in terms of the pulse number  $n$  shows two distinct behaviors, as shown in Fig. 2(a). In this figure, the period of pulse  $\tau$  matches that of the mechanical resonator  $T_0$  ( $\equiv 2\pi/\omega_m$ ) though  $\tau = T_0/k$ , with  $k$  taking the representative values  $\{\frac{1}{2}, 1, 2, 4, 5, 10\}$  denoting the pulse number in one period of the mechanical motion. With  $k \leq 4$ , the QFI  $F$  increases very quickly at the initial pulse number  $n$  and arrives to a large constant value in the large  $n$  limit. However, with the increase of  $k \geq 5$ , the QFI  $F$  shows the behaviors of initially increasing with  $n$  and then gradually going down to zero with large  $n$ . In this case, the value of the QFI is very small compared to that of  $k \leq 4$ . When the pulse period doesn't match the mechanical period, e.g.,  $k \equiv \frac{T_0}{\tau}$  is an irrational number, we also find that the value of QFI  $F$  becomes to much more smaller, compared to the periods match case. More importantly, it is shown in Fig. 2(a) that the QFI  $F$  with  $k = 4$  is optimal, and the reason of this optimal will be discussed in Set. III B.

The physics of these behaviors of the QFI  $F$  can be understood as following. Note that the parameter to be estimated is the mechanical frequency  $\omega_m$ . If the period of the driving pulses  $\tau$  matches that of the mechanical period  $T_0$ , the information of  $\omega_m$  can be extracted to the greatest extent. As a result, the value of QFI  $F$  is large necessarily in the matching cases. A constant value of the QFI in the large  $n$  limit origins from the balance between the pulsed driving and the mechanical damping.

The influence of the mechanical decay rate  $\gamma_m$  on the QFI  $F$  is studied in the resonant driving regime, as shown in Fig. 3(a). This figure displays that with the increase of  $\gamma_m$ , the value of  $F$  decreases considerably. Moreover,  $F$  displays the oscillation behavior when  $\gamma_m$  is very small. The reason of this oscillation is simple: the coherent evolution of the mechanical resonator, determined by  $\omega_m$ , is dominated if the mechanics

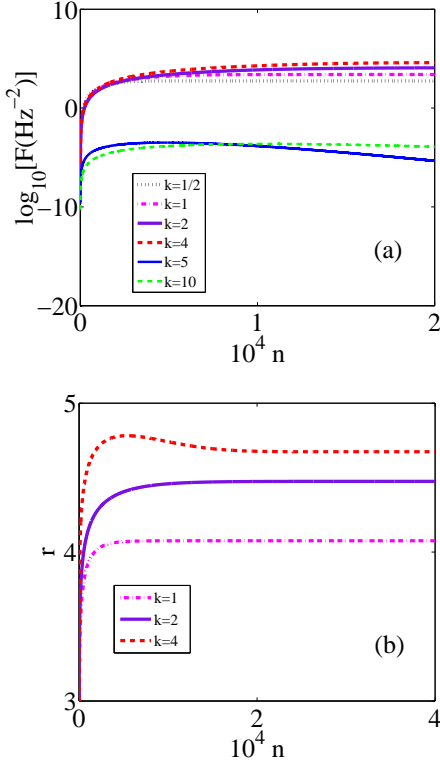


FIG. 2: (Color online) (a) and (b) corresponds to the variation of the QFI  $F$  and the squeezing degree  $r$  defined in Eq. (12) in terms of the pulse number  $n$ , respectively. Different lines corresponds to the different values of the parameter  $k = T_0/\tau$  ( $\tau$  being the period of the pulses and  $T_0 = 2\pi/\omega_m$ ), respectively. The other parameters are  $n_{th} = 100$  and  $\theta = 1.0$ .

has very high quantity factor  $\frac{\omega_m}{\gamma_m}$ .

The effect of the kick strength  $\theta$  on the QFI  $F$  is shown in Fig. 3(b). It is obvious that  $F$  also goes down considerably with the decrease of  $\theta$ . This can be easily understood: without external driving, the mechanical damping will suppress its coherence in the long-time limit. As a result, it is natural that the QFI  $F$  decreases.

In order to show the advantage of our pulsed-driving estimation protocol, we study in Fig. 4(a) the relationship between the growing-up part of the QFI  $F$  and the pulse number  $n$ . We find that  $F \propto n^\alpha$  by numerically fitting, with the index  $\alpha$  dependent on the parameter  $k$ , as shown in Fig. 4(b). Moreover, we also checked numerically that this dependence of  $\alpha$  on  $k$  is independent of the parameters  $\gamma_m$  and  $\theta$ .

From Fig. 4(b), it's clear that the QFI  $F$  with respect to the pulse number  $n$  approaches the Heisenberg limit with  $\alpha = 2$  for the relatively large  $k > 10$ , similar to the results obtained previously in the systems of the pulsed driving qubit [66, 67]. For  $k = 2, 4$ , the QFI shows the behaviour beyond the Heisenberg limit [68] with  $\alpha = 3$ . The Heisenberg limit and beyond it display that the pulsed driving is an essential way to enhance the precision of parameter estimation.

In the following, we discuss how to read out the mechanical

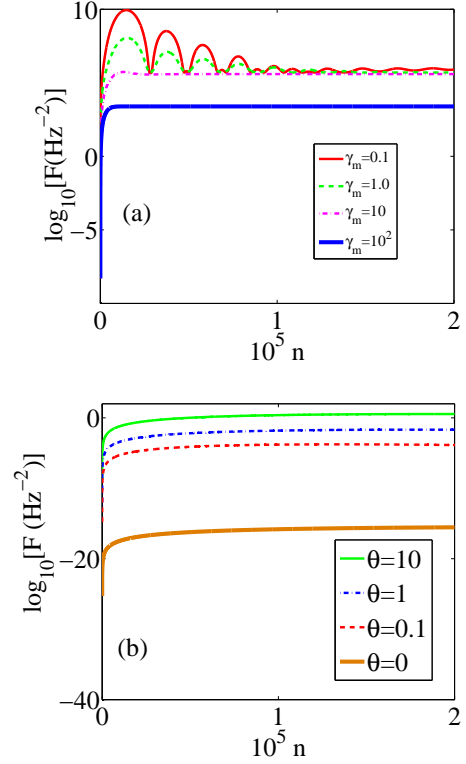


FIG. 3: (Color online) The QFI  $F$  as a function of the pulse number  $n$  with different decay rate  $\gamma_m$  (in units of Hz) for  $\theta = 1.0$  and  $k \equiv T_0/\tau = 1$  and with different kick strength  $\theta$  for  $\gamma_m = 10^2$  Hz and  $\tau = 10^{-7}$  s (b). The other parameter is  $n_{th} = 100$ .

quadratures experimentally, which are required for the QFI of the mechanical resonator. For the pulsed optomechanical system, there exist at least two experimentally feasible schemes to achieve this aim. The main idea of the first one [51] is based on the homodyne detection of the mixing between the signal pulses, which interact with the mechanical resonator, and the local oscillator (LO) pulses, as shown in Ref. [51] (wherein Fig. 1(a)). The second scheme is based on the beam-splitter interaction, where the mechanical quadratures are transferred into the optical readout pulses (latter injected), as displayed in Ref. [49] (wherein Fig. 2). Thus, the information of the mechanical resonator can be gained with the output of the readout pulses.

#### IV. MECHANICAL SQUEEZING AS A QUANTUM RESOURCE

Generally, it is well-known that the squeezed state [70], as an essential resource for quantum metrology [71, 72], can enhance the precision of parameter estimation. Motivated by this fact, we study the relationship between the QFI  $F$  and the mechanical squeezing in this section.

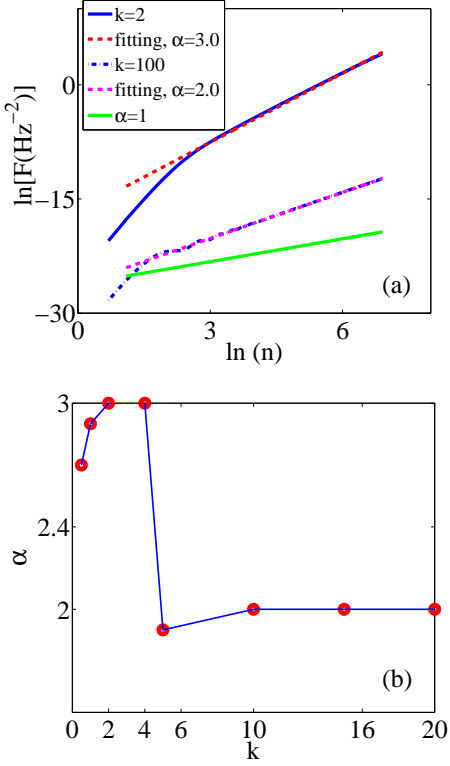


FIG. 4: (Color online) (a) Fitting the growing-up part of  $F$  with respect to the pulse number  $n$ . The index  $\alpha$  is determined by numerically fitting  $F \propto n^\alpha$ . Both the x-axis and y-axis are scaled based on the natural logarithm. The shot-noise limit ( $\alpha = 1$ ) is displayed as the green line. (b) The dependence of the index  $\alpha$  on the parameter  $k$ . The other parameters are the same as that in Fig. 2.

Any single-mode Gaussian state can be expressed as [73]

$$\rho = \hat{D}(\alpha)\hat{S}(r, \phi)\rho_{th}(\bar{n})\hat{S}^\dagger(r, \phi)\hat{D}^\dagger(\alpha), \quad (11)$$

where  $\hat{D}(\alpha) = \exp[\alpha\hat{a} - h.c.]$  is the displacement operator of bosonic mode  $\hat{a}$ ,  $\hat{S}(r, \phi) = \exp[\frac{r}{2}(e^{-2i\phi}\hat{a}^2 - h.c.)]$  is the squeezing operator, and  $\rho_{th}(\bar{n}) = \sum_{m=0}^{\infty} \frac{\bar{n}^m}{(\bar{n}+1)^{m+1}} |m\rangle\langle m|$  denotes the thermal state with  $\bar{n}$  the mean particle number. The squeezing strength  $r$  and the squeezing angle  $\phi$  are determined by

$$r = \frac{1}{2} \text{arcsinh}[\frac{1}{2}(\frac{\gamma}{\det \Sigma_\varphi})^{\frac{1}{2}}], \quad (12)$$

$$2\phi = \begin{cases} -\arcsin(\frac{2\Sigma_{\varphi, 12}}{\sqrt{\gamma}}), & \text{if } \Sigma_{\varphi, 11} < \Sigma_{\varphi, 22}, \\ \pi + \arcsin(\frac{2\Sigma_{\varphi, 12}}{\sqrt{\gamma}}), & \text{if } \Sigma_{\varphi, 11} > \Sigma_{\varphi, 22}, \end{cases} \quad (13)$$

with  $\gamma = (\Sigma_{\varphi, 22} - \Sigma_{\varphi, 11})^2 + (2\Sigma_{\varphi, 12})^2$ . Here  $\Sigma_{\varphi, ij}$  ( $i, j = 1, 2$ ) is the element of the covariant matrix  $\Sigma_\varphi$  as defined in Eq. (A6).

By rearranging the second-order moments given in Eq. (9) as the covariant matrix, the squeezing strength  $r$  and the

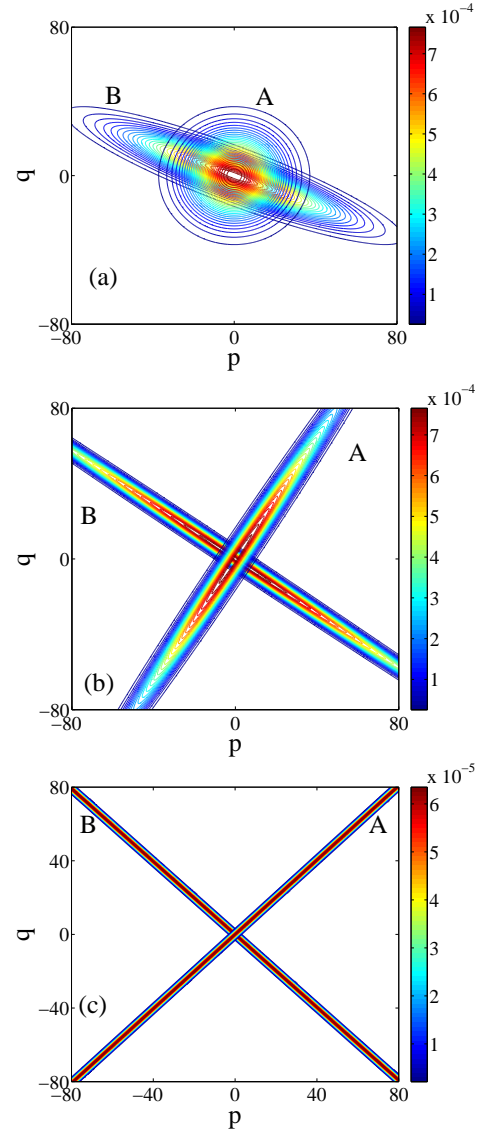


FIG. 5: (Color online) The contour of Wigner functions of the mechanical resonator before (after) the  $n$ -th kicked pulses are labeled as A (B). (a), (b) and (c) corresponds to the pulse number  $n = 1$ ,  $n = 3$  and  $n = 10^3$ , respectively. It is obvious that here the mechanical squeezing can be strengthened by the kicks. The parameters are  $k = 4$ ,  $n_{th} = 100$ , and  $\theta = 1.0$ .

squeezing angle  $\phi$  are obtained according to Eqs. (12) and (13). Note that  $\alpha = 0$  for the mechanical resonator studied in this paper. In Fig. 2(b), we plot the mechanical squeezing strength  $r$  as a function of the pulse number  $n$  for  $k \leq 4$ . By combining Fig. 2(b) and Fig. 2(a), it is apparent that both the mechanical squeezing and the QFI are enhanced with the increase of  $k$ . As a result, this squeezing as a quantum metrology resource strengthens the QFI  $F$ . Although Fig. 2(b) only shows the case  $k \leq 4$ , the similar results have been found for the other  $k$  values (not displayed here).

Based on the correlation between the QFI and the mechanical squeezing, we provide an intuitive way to understand

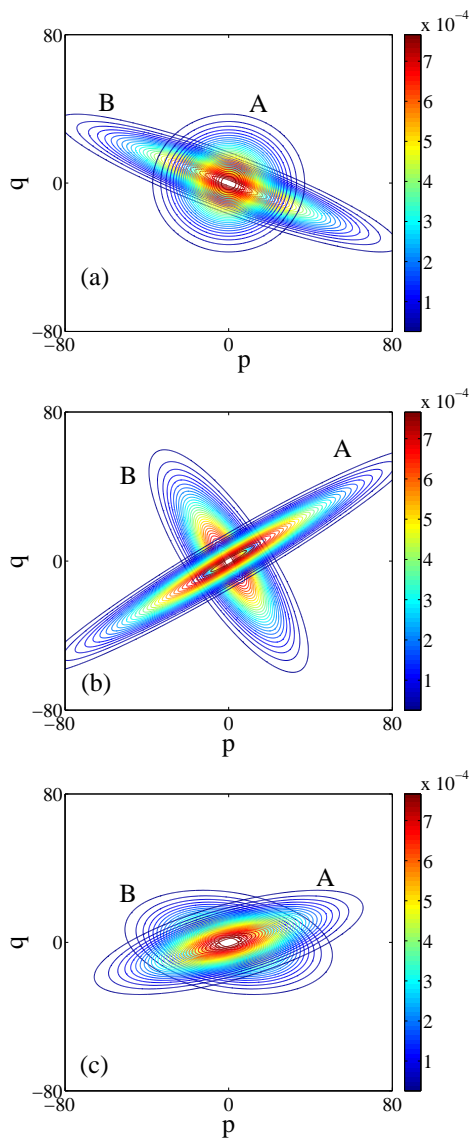


FIG. 6: (Color online) The same to Fig. 5 except for the parameter  $k = 5$ , corresponding to the free rotation angle  $\vartheta = 2\pi/5$ . In this case, the kicks cannot effectively produce the mechanical squeezing.

the QFI for  $k = 4$  (corresponding to a free rotation time  $\tau = T_0/4$ ) being optimal with the kick strength  $\theta = 1$ . To this aim, it is useful to investigate the dynamics of the mechanical Wigner function, obtained according to Eq. (A8).

The kick operator  $\mathbf{K}$  produces the mechanical squeezing, which remains invariant under free rotation  $\mathbf{M}_0(\tau)$  (neglecting the mechanical damping). After the first kick acts on the mechanical resonator, the initial mechanical thermal state translates into a squeezed state with the squeezing angle  $\phi(n = 1) \simeq \pi/8$ , as shown in Fig. 5(a). Here  $\phi$  is defined as the angle between the  $q$ -axis and the direction of the squeezed quadrature. Then, the squeezed state is rotated by  $\vartheta = \omega_m T_0/4 = \pi/2$  along the clockwise direction by the free evolution  $\mathbf{M}_0(\tau = T_0/4)$ . Under the effect of the follow-

ing kicks, the squeezing strength of the mechanical resonator progressively increases, as displayed in Figs. 5(b) and 5(c).

Moreover, the squeezing angle is also gradually approaches to  $\phi \simeq \pi/4$  under some (e.g.,  $n \approx 10^2$ ) repetitive kicks (as well as the free evolution between the kicks). Once the squeezing angle becomes to  $\phi = \pi/4$ , which coincides with the counterpart angle produced by the squeezing action  $\tilde{U}_{\theta=1} = \exp[-i(\hat{a}^2 + h.c.)/2]$  in the kick operator  $U_K$ , we find numerically that it will remain unchanged for large  $n$  limit. We would like to point out that here the matching between the squeezing angle by kick and the free rotation angle plays an essential role in strengthening the mechanical squeezing. As a consequence, the QFI of the mechanical resonator is also enhanced.

We also show the mechanical Wigner function for the case  $k = 5$  in Fig. 6, which corresponds to a free rotation angle  $\vartheta = \omega_m T_0/5 = 2\pi/5$ . Thus, after the free rotation (with considering the mechanical damping) represented by the operator  $\mathbf{M}_0(\tau = T_0/5)$ , the mechanical resonator cannot evolve into the squeezed state with the squeezing angle  $\phi = \pi/4$  by the kick operator  $U_K$  in the long-time limit. This enables the kicks squeeze the mechanical resonator ineffectively, as display in Fig. 6(c).

## V. CONCLUSION

In summary, the quantum pulsed optomechanical system is proposed to apply for the quantum metrology in context of quantum parameter estimation by focusing on investigating the Quantum Fisher information. We find that the mechanical frequency can be estimated with very high precision if the mechanical period matches to that of the driving pulses. We also display that the mechanical squeezing is the quantum resource used in optimal quantum estimation on the frequency. In future, it is an interesting subject to utilize coherence of the multi-mode cavity optomechanics [74, 75] to enhance the accuracy of quantum parameter estimation.

*Acknowledgments.* We thank X. G. Wang, X. W. Xu, H. Fu and X. Xiao for their helpful discussions. This work is supported by the National Natural Science Foundation of China (Grant Nos. 11365006, 11422437, and 11121403, 11565010) and the 973 program (Grants No. 2012CB922104 and No. 2014CB921403), Guizhou province science and technology innovation talent team (Grant No. (2015)4015).

### Appendix A: QFI of a single-mode Gaussian state

In order to keep the completeness of this paper, here we review the main aspects of local quantum estimation theory, especially focusing on the QFI of a single-mode Gaussian state. Note that the mechanical resonator studied in this paper stays in a single-mode Gaussian state.

Let  $\varphi$  denote a single parameter to be estimated, and  $p(\zeta|\varphi)$  be the probability density with measurement outcome  $\{\zeta\}$  for

a continuous observable  $W$  conditioned on the fixed parameter  $\varphi$ . The value of the parameter  $\varphi$  can be inferred from the estimator function  $\hat{\varphi} = \hat{\varphi}(\zeta_1, \dots, \zeta_N)$ , based on the measurement results  $\zeta_1, \dots, \zeta_N$  of  $N$  replicas of the system. Usually, this is achieved by the maximum likelihood estimation. With the definition of the classical Fisher information [76]

$$H_\varphi = \int d\zeta p(\zeta|\varphi) \left[ \frac{\partial}{\partial \varphi} \ln p(\zeta|\varphi) \right]^2, \quad (\text{A1})$$

the classical Cramér-Rao inequality [77] gives the bound of the variance  $\text{Var}(\hat{\varphi})$  for an unbiased estimator  $\hat{\varphi}$

$$\text{Var}(\hat{\varphi}) \geq \frac{1}{H_\varphi}, \quad (\text{A2})$$

Extending from classical to quantum regime, the conditional probability  $p(\zeta|\varphi)$  is determined by positive operator valued measure operator  $\{\hat{E}_\zeta\}$  for a parameterized quantum state  $\rho_\varphi$ ,  $p(\zeta|\varphi) = \text{Tr}[\hat{E}_\zeta \rho_\varphi]$ . To determine the ultimate bound to precision posed by quantum mechanics, the Fisher information must be maximized over all possible measurements [78].

By introducing the symmetric logarithmic derivative  $L_\varphi$  determined by

$$\frac{\partial \rho_\varphi}{\partial \varphi} = \frac{1}{2}(\rho_\varphi L_\varphi + L_\varphi \rho_\varphi),$$

the so-called quantum Cramér-Rao inequality gives a bound to the variance of any unbiased estimator [79]:

$$\text{Var}(\hat{\varphi}) \geq \frac{1}{H_\varphi} \geq \frac{1}{F_\varphi}, \quad (\text{A3})$$

where

$$F_\varphi = \text{Tr}[\rho_\varphi L_\varphi^2] \quad (\text{A4})$$

is the quantum Fisher information.

The two bounds for the precision of parameter estimation [80] have been found, the so-called shot-noise limit  $1/\sqrt{N}$  and the Heisenberg limit  $1/N$ . Usually, here  $N$  is the total particle number contributed to quantum estimation.

It is not easy to give the explicit formula of QFI for a general system. Fortunately, the QFI is related to the Bures distance [79] through

$$D_B^2[\rho_\varphi, \rho_{\varphi+d\varphi}] = \frac{1}{4} F_\varphi d\varphi^2, \quad (\text{A5})$$

where the definition of the Bures distance between two quantum states  $\rho$  and  $\sigma$  is as [81]

$$D_B[\rho, \sigma] = [2(1 - \text{Tr}\sqrt{\rho^{1/2}\sigma\rho^{1/2}})]^{1/2}.$$

The Wigner function for an arbitrary given state  $\rho$ , defined as

$$W(q, p) = \frac{1}{2\pi} \int_{-\infty}^{\infty} ds e^{-ips} \langle q - s | \rho | q + s \rangle,$$

can be used to equivalently represent the corresponding quantum state  $\rho$ , as there is a one-to-one correspondence between them. Gaussian state, as a specific kind of continuous-variable states, has wide applications in actual quantum information processing [82]. They can be reproduced efficiently and unconditionally in the experiment. The unconditionedness is one advantage of the continuous-variable state, which is hard to achieve in the qubit-based discrete-variable.

A state is said to be Gaussian in case its Wigner function is Gaussian. A Gaussian state can be completely characterized by the first-order moment and the second-order moment

$$\begin{aligned} \overline{X_i} &= \langle \hat{X}_i \rangle, \\ \Sigma_{\varphi, ij} &= \frac{1}{2} \langle (\hat{X}_i \hat{X}_j + \hat{X}_j \hat{X}_i) \rangle - \langle \hat{X}_i \rangle \langle \hat{X}_j \rangle \\ &= \int W(\vec{X}) X_i X_j d^2 \vec{X}. \end{aligned} \quad (\text{A6})$$

Here

$$\vec{X} \equiv (\hat{q}, \hat{p}), \quad \langle \dots \rangle \equiv \text{Tr}(\rho_\varphi \dots), \quad (\text{A7})$$

and  $\varphi$  is the parameter to be estimated in the quantum state  $\rho_\varphi$ . The Wigner function is related to the the second-order moments as (setting the first-order moments being zeros)

$$W(\vec{X}) = \frac{1}{2\pi \sqrt{\text{Det} \Sigma_\varphi}} \exp(-\frac{1}{2} \vec{X} \Sigma_\varphi^{-1} \vec{X}^T). \quad (\text{A8})$$

Based on the fidelity between arbitrary single-mode Gaussian states  $\rho_1$  and  $\rho_2$ ,

$$f(\rho_1, \rho_2) = \frac{2 \exp[-\frac{1}{2} \Delta X^T (\Sigma_1 + \Sigma_2)^{-1} \Delta X]}{\sqrt{|\Sigma_1 + \Sigma_2| + (1 - |\Sigma_1|)(1 - |\Sigma_2|)} \sqrt{(1 - |\Sigma_1|)(1 - |\Sigma_2|)}}, \quad (\text{A9})$$

making use of Eq. (A5), the QFI of the single-mode Gaussian state is found to be [83, 84]

$$F_\varphi = \frac{\text{Tr}[(\Sigma_\varphi^{-1} \Sigma_\varphi'^2)]}{2(1 + P_\varphi^2)} + 2 \frac{P_\varphi'^2}{1 - P_\varphi^4} + \Delta \vec{X}'^T \Sigma_\varphi^{-1} \Delta \vec{X}'. \quad (\text{A10})$$

Here  $\Delta \vec{X} = \langle \vec{X}_1 - \vec{X}_2 \rangle$  is the mean relative displacement,  $P_\varphi = |\Sigma_\varphi|^{-1/2}$  denotes the purity of the state, and

$$\Delta \vec{X}'_\varphi = d \langle \vec{X}_{\varphi+\epsilon} - \vec{X}_\varphi \rangle / d\epsilon|_{\epsilon=0}. \quad (\text{A11})$$

We notice that the quantum Cramér-Rao bound of two-mode Gaussian states [85] was investigated previously.

- 
- [1] V. Giovannetti, S. Lloyd and L. Maccone, *Science* **306**, 1330 (2004); V. Giovannetti, S. Lloyd and L. Maccone, *Phys. Rev. Lett.* **96**, 010401 (2006); V. Giovannetti, S. Lloyd, and L. Maccone, *Nat. Photonics* **5**, 222 (2011).
- [2] L. Pezzé and A. Smerzi, *Phys. Rev. Lett.* **102**, 100401 (2009); A. Smerzi, *Phys. Rev. Lett.* **109**, 150410 (2012).
- [3] X. M. Lu, X. G. Wang, and C. P. Sun, *Phys. Rev. A* **82**, 042103 (2010); W. Zhong, Z. Sun, J. Ma, X. G. Wang, and F. Nori, *Phys. Rev. A* **87**, 022337 (2013); Q. S. Tan, Y. X. Huang, X. L. Yin, L. M. Kuang, and X. G. Wang, *Phys. Rev. A* **87**, 032102 (2013).
- [4] Y. Yao, L. Ge, X. Xiao, X. G. Wang, and C. P. Sun, *Phys. Rev. A* **90**, 022327 (2014).
- [5] Y. M. Zhang, X. W. Li, W. Yang, and G. R. Jin, *Phys. Rev. A* **88**, 043832 (2013).
- [6] Q. Zheng, L. Ge, Y. Yao, and Q. J. Zhi, *Phys. Rev. A* **91**, 033805 (2015).
- [7] T. Nagata, R. Okamoto, J. L. O'Brien, K. Sasaki, and S. Takeuchi, *Science* **316**, 726 (2007).
- [8] I. Afek, O. Ambar, and Y. Silberberg, *Science* **328**, 879 (2010).
- [9] F. Hudelist, J. Kong, C. Liu, J. Jing, Z. Y. Ou, and W. P. Zhang, *Nat. Commun.* **5**, 3049 (2014).
- [10] H. Strobelt, W. Muessel, D. Linnemann, T. Zibold, D. B. Hume, L. Pezzè, A. Smerzi, and M. K. Oberthaler, *Science* **345**, 424 (2014).
- [11] W. D. Li, T. C. He, and A. Smerzi, *Phys. Rev. Lett.* **113**, 023003 (2014).
- [12] G. Q. Liu, Y. R. Zhang, Y. C. Chang, J. D. Yue, H. Fan, X. Y. Pan, *Nat. Commun.* **6**, 6726 (2015).
- [13] N. Zhao and Z. Q. Yin, *Phys. Rev. A* **90**, 042118 (2014).
- [14] K. Iwasawa, K. Makino, H. Yonezawa, M. Tsang, A. Davidovic, E. Huntington, and A. Furusawa, *Phys. Rev. Lett.* **111**, 163602 (2013).
- [15] S. Z. Ang, G. I. Harris, W. P. Bowen, and M. Tsang, *New J. Phys.* **15**, 103028 (2013).
- [16] M. Tsang, *New J. Phys.* **15**, 073005 (2013).
- [17] T. J. Kippenberg and K. J. Vahala, *Science* **321**, 1172 (2008).
- [18] M. Aspelmeyer, P. Meystre, and K. C. Schwab, *Phys. Today*, **65**, 29 (2012); P. Meystre, *Ann. Phys. (Berlin)* **525**, 215 (2013).
- [19] M. Aspelmeyer, T. J. Kippenberg, and F. Marquardt, *Cavity Optomechanics* (Springer-Verlag Berlin Heidelberg, 2014).
- [20] M. Aspelmeyer, T. J. Kippenberg, and F. Marquardt, *Rev. Mod. Phys.* **86**, 1391 (2014).
- [21] L. F. Buchmann, L. Zhang, A. Chiruvelli, and P. Meystre *Phys. Rev. Lett.* **108**, 210403 (2012); H. T. Tan, F. Bariani, G. X. Li, and P. Meystre, *Phys. Rev. A* **88**, 023817 (2013).
- [22] W. Marshall, C. Simon, R. Penrose, and D. Bouwmeester, *Phys. Rev. Lett.* **91**, 130401 (2003).
- [23] F. Xue, Y. X. Liu, C. P. Sun, and F. Nori, *Phys. Rev. B* **76**, 064305 (2007).
- [24] D. Rugar, R. Budakian, H. J. Mamin, and B. W. Chui, *Nature (London)* **430**, 329 (2004); A. G. Krause, M. Winger, T. D. Blasius, Q. Lin, and O. Painter, *Nat. Photon.* **6**, 768 (2012).
- [25] C. A. Regal, J. D. Teufel, and K. W. Lehnert, *Nat. Phys.* **4**, 555 (2008).
- [26] J. D. Teufel, T. Donner, M. A. Castellanos-Beltran, J. W. Harlow, and K. W. Lehnert, *Nat. Nanotechnol.* **4**, 820 (2009).
- [27] S. Forstner, S. Prams, J. Knittel, E. D. van Ooijen, J. D. Swaim, G. I. Harris, A. Szorkovszky, W. P. Bowen, and H. Rubinsztein-Dunlop, *Phys. Rev. Lett.* **108**, 120801 (2012).
- [28] X. Xu and J. M. Taylor, *Phys. Rev. A* **90**, 043848 (2014).
- [29] A. Arvanitaki and A. A. Geraci, *Phys. Rev. Lett.* **110**, 071105 (2013).
- [30] S. Mancini, D. Vitali, and P. Tombesi, *Phys. Rev. Lett.* **90**, 137901 (2003).
- [31] Sh. Barzanjeh, S. Guha, C. Weedbrook, D. Vitali, J. H. Shapiro, and S. Pirandola, *Phys. Rev. Lett.* **114**, 080503 (2015).
- [32] S. Weis, R. Rivière, S. Deléglise, E. Gavartin, O. Arcizet, A. Schliesser, and T. J. Kippenberg, *Science* **330**, 1520 (2010); A. H. Safavi-Naeini, T. P. M. Alegre, J. Chan, M. Eichenfield, M. Winger, Q. Lin, J. T. Hill, D. E. Chang, and O. Painter, *Nature (London)* **472**, 69 (2011).
- [33] G. S. Agarwal and S. Huang, *Phys. Rev. A* **81**, 041803(R) (2010).
- [34] I. Wilson-Rae, N. Nooshi, W. Zwerger, and T. J. Kippenberg, *Phys. Rev. Lett.* **99**, 093901 (2007); F. Marquardt, J. P. Chen, A. A. Clerk, and S. M. Girvin, *ibid.* **99**, 093902 (2007).
- [35] C. Genes, D. Vitali, P. Tombesi, S. Gigan, and M. Aspelmeyer, *Phys. Rev. A* **77**, 033804 (2008).
- [36] J. D. Teufel, T. Donner, D. Li, J. H. Harlow, M. S. Allman, K. Cicak, A. J. Sirois, J. D. Whittaker, K. W. Lehnert, and R. W. Simmonds, *Nature (London)* **475**, 359 (2011).
- [37] Y. J. Guo, K. Li, W. J. Nie, and Y. Li, *Phys. Rev. A* **90**, 053841 (2014).
- [38] J. Chan, T. P. Mayer Alegre, A. H. Safavi-Naeini, J. T. Hill, A. Krause, S. Groblacher, M. Aspelmeyer and O. Painter, *Nature* **478**, 89 (2011).
- [39] M. Paternostro, D. Vitali, S. Gigan, M. S. Kim, C. Brukner, J. Eisert, and M. Aspelmeyer, *Phys. Rev. Lett.* **99**, 250401 (2007); Sh. Barzanjeh, M. Abdi, G. J. Milburn, P. Tombesi, and D. Vitali, *Phys. Rev. Lett.* **109**, 130503 (2012).
- [40] L. Tian, *Phys. Rev. Lett.* **110**, 233602 (2013); Y. D. Wang and A. A. Clerk, *ibid.* **110**, 253601 (2013).
- [41] W. Wiczcerek, S. G. Hofer, J. Hoelscher-Obermaier, R. Riedinger, K. Hammerer, and M. Aspelmeyer, *Phys. Rev. Lett.* **114**, 223601 (2015).
- [42] M. R. Vanner, I. Pikovski, G. D. Cole, M. S. Kim, Č. Bruknera, K. Hammerer, G. J. Milburn, and M. Aspelmeyer, *Proc. Natl. Acad. Sci. USA* **108**, 16182 (2011).
- [43] L. Viola and S. Lloyd, *Phys. Rev. A* **58**, 2733 (1998).
- [44] K. Hammerer, E. S. Polzik, and J. I. Cirac, *Phys. Rev. A* **72**, 052313 (2005).
- [45] O. Romero-Isart, A. C. Pflanzer, M. L. Juan, R. Quidant, N. Kiesel, M. Aspelmeyer, and J. I. Cirac, *Phys. Rev. A* **83**, 013803 (2011).
- [46] M. Asjad, G. S. Agarwal, M. S. Kim, P. Tombesi, G. Di Giuseppe, and D. Vitali, *Phys. Rev. A* **89**, 023849 (2014).
- [47] J. Q. Liao and C. K. Law, *Phys. Rev. A* **84**, 053838 (2011).
- [48] S. G. Hofer, W. Wiczcerek, M. Aspelmeyer, and K. Hammerer, *Phys. Rev. A* **84**, 052327 (2011).
- [49] T. A. Palomaki, J. D. Teufel, R. W. Simmonds, K. W. Lehnert, *Science* **342**, 710 (2013).
- [50] Q. Y. He, and M. D. Reid, *Phys. Rev. A* **88**, 052121 (2013); S. Kiesewetter, Q. Y. He, P. D. Drummond, and M. D. Reid, *Phys. Rev. A* **90**, 043805 (2014).
- [51] M. R. Vanner, J. Hofer, G. D. Cole, and M. Aspelmeyer, *Nat. Commun.* **4**, 2295 (2013).
- [52] S. Machnes, J. Cerrillo, M. Aspelmeyer, W. Wiczcerek, M. B. Plenio, and A. Retzker, *Phys. Rev. Lett.* **108**, 153601 (2012).
- [53] O. Arcizet, P. F. Cohadon, T. Briant, M. Pinard, A. Heidmann, *Nature (London)* **444**, 71 (2006).
- [54] G. Anetsberger, O. Arcizet, Q. P. Unterreithmeier, R. Rivière,



- A. Schliesser, E. M. Weig, J. P. Kotthaus, and T. J. Kippenberg, *Nat. Phys.* **5**, 909 (2009).
- [55] N. Kiesel, F. Blaser, U. Delić, D. Grass, R. Kaltenbaek, and M. Aspelmeyer, *Proc. Natl. Acad. Sci. USA* **110**, 14180 (2013).
- [56] T. P. Purdy, D. W. C. Brooks, T. Botter, N. Brahms, Z.-Y. Ma, and D. M. Stamper-Kurn, *Phys. Rev. Lett.* **105**, 133602 (2010).
- [57] J. C. Sankey, C. Yang, B. M. Zwickl, A. M. Jayich, and J. G. E. Harris, *Nat. Phys.* **6**, 707 (2010).
- [58] J. D. Thompson, B. M. Zwickl, A. M. Jayich, F. Marquardt, S. M. Girvin, J. G. E. Harris, *Nature (London)* **452**, 72 (2008).
- [59] Z. J. Deng, Y. Li, M. Gao, and C. W. Wu, *Phys. Rev. A* **78**, 032303 (2008).
- [60] G. Heinrich, J. G. E. Harris, F. Marquardt, *Phys. Rev. A* **81**, 011801 (2010); H. Z. Wu, G. Heinrich, and F. Marquardt, *New J. Phys.* **15**, 123022(2013).
- [61] T. K. Paraiso, M. Kalaee, L. Zang, H. Pfeifer, F. Marquardt, and O. Painter, *Phys. Rev. X* **5**, 041024 (2015).
- [62] M. Bhattacharya and P. Meystre, *Phys. Rev. Lett.* **99**, 073601 (2007); M. Bhattacharya, H. Uys, and P. Meystre, *Phys. Rev. A* **77**, 033819 (2008).
- [63] A. Nunnenkamp, K. Børkje, J. G. E. Harris, and S. M. Girvin, *Phys. Rev. A* **82**, 021806(R) (2010).
- [64] J. J. Li and K. D. Zhu, *Phys. Rep.* **525**, 223 (2013).
- [65] N. E. Flowers-Jacobs, S. W. Hoch, J. C. Sankey, A. Kashkanova, A. M. Jayich, C. Deutsch, J. Reichel, and J. G. E. Harris, *Appl. Phys. Lett.* **101**, 221109 (2012).
- [66] Y. Watanabe, T. Sagawa, and M. Ueda, *Phys. Rev. Lett.* **104**, 020401 (2010).
- [67] Q. S. Tan, Y. X. Huang, X. L. Yin, L. M. Kuang, and X. G. Wang, *Phys. Rev. A* **87**, 032102 (2013).
- [68] S. Boixo, A. Datta, S. T. Flammia, A. Shaji, E. Bagan, and C. M. Caves, *Phys. Rev. A* **77**, 012317 (2008); Y. C. Liu, G. R. Jin, and L. You, *Phys. Rev. A* **82**, 045601 (2010).
- [69] C. W. Gardiner and P. Zoller, *Quantum Noise* (Springer, New York, 2000).
- [70] J. Ma, X. G. Wang, C. P. Sun, and F. Nori, *Phys. Rep.* **509**, 89 (2011).
- [71] C. M. Caves, *Phys. Rev. D* **23**, 1693 (1981); M. D. Lang and C. M. Caves, *Phys. Rev. Lett.* **111**, 173601 (2013).
- [72] L. Pezzé and A. Smerzi, *Phys. Rev. Lett.* **110**, 163604 (2013).
- [73] C. Weedbrook, S. Pirandola, R. Garcia-Patron, N. J. Cerf, T. C. Ralph, J. H. Shapiro, and S. Lloyd, *Rev. Mod. Phys.* **84**, 621 (2012).
- [74] X. W. Xu, Y. J. Zhao, and Y. X. Liu, *Phys. Rev. A* **88**, 022325 (2013).
- [75] F. Massel, S. U. Cho, J. M. Pirkkalainen, P. J. Hakonen, T. T. Heikkilä, and M. Sillanpää, *Nat. Commun.* **3**, 987 (2012).
- [76] R. A. Fisher, *Proc. Cambridge Philos. Soc.* **22**, 700 (1925).
- [77] A. S. Holevo, *Probabilistic and Statistical Aspects of Quantum Theory* (North-Holland, Amsterdam, 1982).
- [78] M. G. A. Paris, *Int. J. Quant. Inf.* **7**, 125 (2009).
- [79] S. L. Braunstein and C. M. Caves, *Phys. Rev. Lett.* **72**, 3439 (1994).
- [80] S. L. Braunstein, C. M. Caves, and G. J. Milburn, *Ann. Phys. (N.Y.)* **247**, 135 (1996).
- [81] M. A. Nielsen and I. L. Chuang, *Quantum Computation and Quantum Information* (Cambridge University Press, Cambridge, U.K., 2000).
- [82] A. Ferraro, S. Olivares, and M. G. A. Paris, *Gaussian States in Quantum Information*, Napoli Series on Physics and Astrophysics (Bibliopolis, Napoli, 2005).
- [83] O. Pinel, P. Jian, N. Treps, C. Fabre, and D. Braun, *Phys. Rev. A* **88**, 040102 (2013).
- [84] D. D. de Souza, M. G. Genoni, M. S. Kim, *Phys. Rev. A* **90**, 042119(2014).
- [85] M. G. Genoni, P. Giorda, and M. G. A. Paris, *Phys. Rev. A* **78**, 032303 (2008); X. X. Zhang, Y. X. Yang, and X. B. Wang, *Phys. Rev. A* **88**, 013838 (2013).